19th Brazilian Congress of Thermal Sciences and Engineering
November 06th-10th, 2022, Bento Gonçalves - RS - Brazil

ENC-2022-0172

DEALING WITH STAIRCASE GEOMETRIES IN THE NUMERICAL ANALYSIS OF HEAT TRANSFER FROM CURVED SURFACES BY THE LATTICE BOLTZMANN METHOD

Evani Mollossi Porto
Pontifical University Catholic of Parana PUC-PR, rua Imaculada Conceição 1155, Prado Velho, Curitiba, PR, Brazil
evani.mollossi@gmail.com
Stephan Hennings Och
Federal University of Parana – UFPR, rua Cel. Francisco Heráclito dos Santos, 100 - Jardim das Américas, Curitiba, PR, Brazil
stephan.hennings.och@gmail.com

Paulo Cesar Philippi
Pontifical University Catholic of Parana PUC-PR, rua Imaculada Conceição 1155, Prado Velho, Curitiba, PR, Brazil
philippi@Impt.ufsc.br,

Abstract:
In Purpose – The LBM (Lattice Boltzmann Method) is adopted to numerically simulate and calculate the heat exchange coefficients for single cylinders and a bank of aligned and staggered cylinders. The different layouts are evaluated, to verify the gain in the global heat exchange coefficient.
Design/methodology/approach – The method is applied for an incompressible flow, with the employment of the Bhatnagar Gross and Krook (BGK) local collision operator, in a D2Q9 scheme. The computational code is applied for intermediate Reynolds (Re) numbers using a passive-scalar approach for the transport of energy.
Findings – The thermal analysis is performed around the obstacles with the calculation of the local and average Nusselt numbers. The results are compared with available data from experimental and computational works. Errors were found to have the same order of magnitude as the dispersion errors between available data.
Practical implications – Fluid flow and heat transfer across a bank or bundle of cylinders are relevant for several industrial applications, such as steam generation for boilers or coils applied on air conditioner systems. Normally there is an internal flow inside a tube and a second fluid, with a different temperature, flows externally to perform the heat exchange. In these applications with a bundle of cylinders, the overall heat exchange coefficient is desired to be calculated.
Originality/value – Due to its intrinsic cartesian geometry, the use of an LB passive scalar approach for finding the isotherms around curved surfaces requires dealing with staircase geometries. Results show that the method that is proposed in this paper is suitable for evaluating the angular distribution of the local heat transfer coefficient in the range of intermediate Reynolds numbers.

Key words: Heat transfer, lattice-Boltzmann passive-scalar, bank of cylinders.

1. INTRODUCTION

The heat exchange across a bank or bundle of cylinders is important for several industrial applications such as heat exchangers in air conditioning systems Sayehvand, Yari and Basiri (2018). The great variety of applications has motivated research interest for decades, Hsu and Liang (2021).

Solving analytically the Navier–Stokes equations has been a challenge for almost two centuries, since only a few analytical solutions, generally for very simple flows and geometries, are known. The alternative to the formal methodology is to resort to numerical methods, usually discretizing, in several different ways, the Navier–Stokes equations.

In this regard, the lattice Boltzmann equation (LBE) has been successfully used in the last decades as a computational fluid dynamics tool, solving a discrete analog of the Boltzmann equation for the mass, momentum, and energy balance equations. Chen and Doolen (1998), He and Luo (1997). The LBE has proved to be valuable in solving simple and complex flows, Zhou, Dong, Chen and Li (2019).

To assist in the thermodynamic analysis of these components, computational flow simulations in LBM (Lattice Boltzmann Method) have been used as an alternative to traditional CFD methods. Based on microscopic models and mesoscopic kinetic equations, the scheme showed to be successful in applications involving interfacial dynamics and complex boundaries. The central idea of this kinetic model to simulate macroscopic fluid flows is that the macroscopic dynamics of the fluid is the result of the collective behavior of many microscopic particles, Chen and Doolen (1998).

In this method, the fluid is considered as a set of particles, which are propagated along directions (lattice links) and collide at nodes (lattice sites). Although the LBM method is based on a system of particles, its focus is on the average macroscopic behavior, where the kinetic equations provide advantages compared to CFD methods such as easy implementation and use of algorithms that allow parallel execution, Chen and Doolen (1998), Surmas, Dos Santos and Philippi (2004).

Studies regarding the non-isothermal flow past cylinder were carried out with the application of LBM by Zu et al. (2008) and Zhou et al. (2019). In their studies, a numerical simulation of flow with heat exchange is carried out. The results for heat transfer and velocity field in evolution with time, lift, and drag coefficients show excellent agreement with theoretical, experimental, and numerical studies. In both analyses, the LBM method is validated to simulate heat transfer. It was verified a fluctuation of the Nusselt number in the region of rear stagnation of the cylinder, which is gradually increased with the approximation of the isothermal lines. For a bank of cylinders, Esfahani and Vasel-Be-Hagh (2012) investigated the heat transfer for a bundle of 4 cylinders in an aligned layout, and a good agreement with theoretical, experimental, and numerical studies was found. Although both studies have obtained good results, the way to obtain the Nusselt number is not deeply discussed.

In fact, due to its intrinsic cartesian nature, curved surfaces are represented by a staircase geometry in LBM. On the other hand, the calculation of the Nusselt number for a curved surface requires locally evaluating the temperature gradient at the surface and this can reveal to be a difficult task in staircase geometries. In this work, a computational fluid flow simulation code is developed. The LB method is adopted to numerically simulate and to calculate aerodynamic drag and heat exchange coefficients in a bank of tubes. The method is applied for an incompressible fluid and single-phase fluid, with the employment of the BGK local collision operator Bhatnagar, Gross and Krook (1954), in a D2Q9 scheme. The computational code is applied for Reynolds (Re) numbers ranging between 10 and 120 for single cylinders.

Thermal analysis is performed around the obstacles with the calculation of the local and average Nusselt numbers. For a single-cylinder, the simulation is performed with Reynolds varying from 10 to 120. For a bank of 4 cylinders in aligned and staggered layouts, the Reynolds number is set to 80 and 120. The results obtained are compared with average results of experimental and computational works, carried out by different authors and methods. It was found a good agreement on the results and when comparing the aligned and staggered layouts for a bank of four cylinders, a gain of around 30% in the heat exchange factor is also observed.

2. BULK FLOW

A lattice-Boltzmann equation (LBE) may be considered as a special discrete form of the continuous Boltzmann equation, where the molecular velocity space ξ^{D} is replaced by a set of b discrete velocities ξ_i, $i = 0, ..., b-1$ and the continuous distribution function $f(\mathbf{x}, \xi, t)$ is replaced by b packets of particles $fi(\mathbf{x}, t) = f(\mathbf{x}, \xi_i, t)$. Parameter b is related to the order of approximation of the Boltzmann equation. In dimensionless variables, the LBE may be written in terms of the dimensionless populations $f_i = fi\xi^{D}/n_0$ in two parts corresponding to the collision

$$\bar{f}_i'(\mathbf{x}, t+\delta) = \bar{f}_i(\mathbf{x}, t) + \overline{\Omega_i}\,, \tag{1}$$

and propagation steps,

$$\bar{f}_i(x + e_i h, t + \delta) = \bar{f}_i'(x, t + \delta). \tag{2}$$

In Eq. (1)

$$\bar{\Omega}_i = \frac{\bar{f}_i^{eq} - \bar{f}_i}{\tau^*}, \tag{3}$$

is the BGK relaxation term, Bhatnagar et al. (1954) and means that, in the collision step, populations $\bar{f}_i$ that were streamed to point **x** are redistributed along the directions e_i, relaxing to their equilibrium values given by $\bar{f}_i^{eq}$ in accordance with a dimensionless relaxation time $\tau*$. Symbol $\bar{\xi}$ is an average molecular speed and n_0 is a reference number density of particles. Symbol $\mathbf{e}_i$ design the lattice vectors given by $\mathbf{e}_i = \xi_i/c$ where $c = h/\delta$, h being the orthogonal distance between any two contiguous sites and δ the simulation time-step. Figure 1 shows the Hermitian basis and the set of lattice-vectors **e***i* of the D2Q9 second-order LBE.

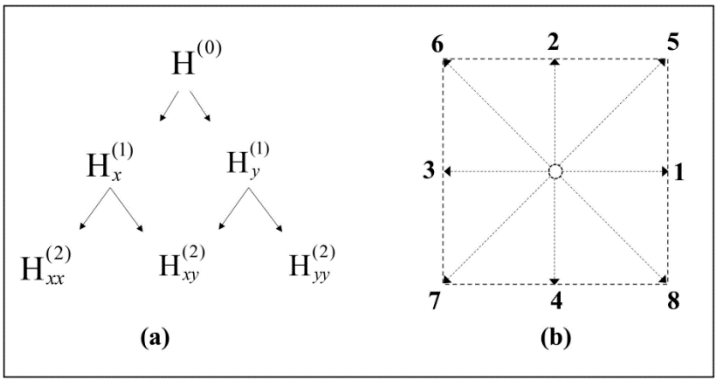

Figure 1: Hermitian representation (a) and set of lattice vectors (b) for the D2Q9 LBE

During simulation, the dimensionless density ρ^* and macroscopic velocity $\mathbf{u}^*$ are updated following

$$\rho^* = \sum_i \bar{f}_i = \sum_i \bar{f}_i^{eq}. \tag{4}$$

$$\rho^* \boldsymbol{u}^* = \sum_i \bar{f}_i \boldsymbol{e}_i = \sum_i \bar{f}_i^{eq} \boldsymbol{e}_i \tag{5}$$

respectively.

In Eqs. (4) and (5), ρ^* and $\mathbf{u}^*$ are required to be equilibrium moments, being necessary conditions for the solvability of the LB numerical scheme. We restrict ourselves to a second-order Hermitian expansion of the Maxwell-Boltzmann equilibrium distribution. In its discrete form it reads as

$$\bar{f}_i^{eq} = W_i \rho^* \left[1 + \frac{u_\infty^* e_{i\alpha}}{c_s^2} + \frac{1}{2} \frac{u_\infty^* u_\beta^*}{c_s^{*4}} \left(e_{i\alpha} e_{i\beta} - c_s^{*2} \delta_{\alpha\beta} \right) \right], \tag{6}$$

where W_i are quadrature weights and c_s is a lattice constant that is related to the speed of sound.

2.1 Non-isothermal flows

When the flow patterns are not affected by the temperature, we can consider the thermal energy as a scalar quantity that is transported along the streamlines by advection and is redistributed among the molecules by collisions. Therefore, a suitable BGK kinetic model for the thermal energy would be written as, He, Chen and Doolen (1998),

$$\partial_t g + \xi_\beta \partial_\beta g = \frac{g^{eq} - g}{\tau}, \tag{7}$$

where g is the internal energy of the particles in a volume element $d\mathbf{x}$ around the position $\mathbf{x}$ and with velocities between ξ and $\xi + d\xi$. The equilibrium distribution is given by

$$g^{eq} = \frac{1}{(2\pi)^{\frac{D}{2}}} \frac{\varepsilon}{\bar{\xi}^D} e^{-\frac{(\xi - \mathbf{u})^2}{2\bar{\xi}^2}}, \tag{8}$$

where,

$$\bar{\xi} = \sqrt{\frac{kT_0}{m}}, \tag{9}$$

is a mean molecular speed at a reference temperature T_0 , k is the Boltzmann constant and m is a molecular mass. The internal energy is, thus, required to be an equilibrium moment

$$\varepsilon = \int g d\xi = \int g^{eq} d\xi . \tag{10}$$

In the collision step, the thermal energy is redistributed among the particles following

$$\bar{g}_i^{'}(\mathbf{x}, t + \delta) = \bar{g}_i(\mathbf{x}, t) + \bar{\Omega}_i^g, \tag{11}$$

and, in the propagation step, this thermal energy is transported with the particles to the neighbor sites

$$\bar{g}_i^{'}(\mathbf{x}+e_i h, t+\delta) = \bar{g}_i^{'}(\mathbf{x}, t+\delta)\,. \tag{12}$$

The collision term is now written as

$$\bar{\Omega}_i^g = \frac{\bar{g}_i^{eq} - \bar{g}_i}{\tau_q^*}, \tag{13}$$

where τ_q^* is a dimensionless relaxation time that is related to the thermal diffusivity and

$$\bar{g}_i^{eq} = W_i \varepsilon^* \left[1 + \frac{(e_{i\alpha} u_\infty^*)}{c_s^2} + \frac{u_\infty^* u_\beta^*}{2c_s^{*2}} \left(\frac{(e_{i\alpha} e_{i\beta})}{c_s^2} - \delta_{\alpha\beta} \right) \right], \tag{14}$$

is the second-order Hermite polynomial expansion of the MB equilibrium distribution given by Eq. (8).

Parameter ε^* is the ratio,

$$\varepsilon^* = \frac{\varepsilon}{\varepsilon_0}, \tag{15}$$

between the internal energy ε ($\mathbf{x}$, t) and a reference value ε_0 . Since $\varepsilon = 3/2nkT$ and $\varepsilon_0 = 3/2\ n_0 kT_0$, this ratio gives

$$\varepsilon^* = \rho^* \theta. \tag{16}$$

It does give the dimensionless temperature $\theta = T/T0$ for ideal gases, which follows the Clapeyron equation of state. Therefore, while, in the course of the simulation, Eqs. (4) and (5) are used to update the density and momentum, respectively, and the local dimensionless temperature is updated following

$$\rho^* \theta = \sum_i \bar{g}_i \tag{17}$$

3. BOUNDARY CONDITIONS

Dealing with boundary conditions (BC) was ever considered a puzzling question in the Lattice-Boltzmann (LB) method. The main question to be solved is how to deal with a problem when the number of unknowns (the particle populations coming from the outside part of the numerical domain) is greater than the number of equations at our disposal at each boundary site.

3.1 Fluid-solid interaction

In this section, it will be explained the interaction between the bulk flow and solid boundaries.

3.1.1 Non-slip boundary condition

The standard half-way bounce-back (HWBB) model is used for representing the fluid-solid interaction. This model is illustrated in Figure 2 and given by

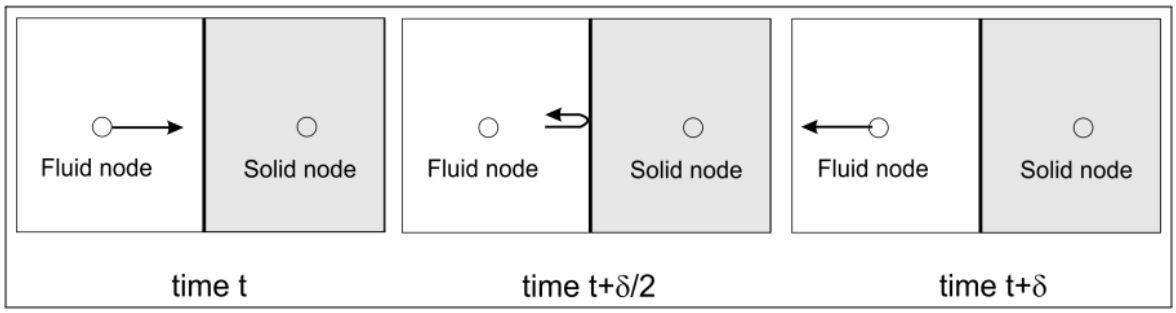

Figure 2: Half-way bounce-back boundary condition for fluid-solid interaction.

$$\overline{f}_{-i}(\boldsymbol{x}_b, t+\delta) = \overline{f}_i\left(\boldsymbol{x}_b, t\right), \tag{18}$$

for all directions i pointing to a solid surface, from the boundary node $\mathbf{x}_b$. Therefore, the solid surface is supposed to be in an intermediate position between the fluid boundary node and the solid node in the neighboring. The population $\overline{f}_i\left(x_b, t\right)$ that is present in this site $\mathbf{x}b$ at time step t, with a velocity $\mathbf{e}i$ pointing to the solid, is considered to rebound on this surface and return to the boundary node with an inverted velocity at time $t + \delta$.

The standard bounce-back boundary condition is mass preserving and can be used for moving surfaces (Ladd, 1994), but cannot prevent slip when applied to corners. On the other hand in its halfway version, the location of the zero-slip point is dependent on the fluid viscosity. Nonetheless, it is the most frequently used model for fluid-solid interaction. Its main advantage is its simplicity and easiness to be implemented. Interested readers are suggested to read (Bazarin et al., 2021) where other alternatives are presented and discussed.

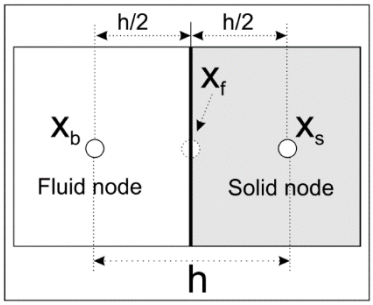

Figure 3: Half-way bounce back boundary condition for the energy distribution.

3.1.2 Energy redistribution at the wall

Consider Figure 3. Nodes $\mathbf{x}_b$ and $\mathbf{x}_s$ are, respectively, the boundary node at the fluid phase and a fictive node in the solid phase. The solid surface is located in the halfway, $\mathbf{x}_f$, between these two nodes, where the dimensionless temperature is θ. Since this solid surface is at rest, we can use Eq. (14) to find the energy amount $\overline{g}_i^{eq} = \rho^* W_i \theta$ at this node, related to an arbitrary direction i. We further suppose that this energy amount is the arithmetic average of the energy amount that comes from node $\mathbf{x}b$ in the fluid phase and the one that comes from the fictive solid node $\mathbf{x}_s$

$$\frac{\bar{g}_1(\boldsymbol{x}_b,t)+\bar{g}_3(\boldsymbol{x}_s,t)}{2}=\rho^* W(|e_i=1|)\theta, \tag{19}$$

and based on the HWBB BC, the particles that come from the solid node $\mathbf{x}_s$ are in fact the ones that rebounded in the wall, returning to the site $\mathbf{x}_b$ at time $t+\delta$

$$\bar{g}_3(\boldsymbol{x}_s,t)=\bar{g}_3(\boldsymbol{x}_b,t+\delta) \tag{20}$$

Eqs. (19) and (20) can be generalized for all directions pointing to the solid surface as

$$\frac{\bar{g}_i(\boldsymbol{x}_b,t)+\bar{g}_{-i}(\boldsymbol{x}_b,t+\delta)}{2}=\rho^* W_i\theta \tag{21}$$

Eq. (21) was proposed by Zhang, Shi, Guo, Chai and Lu (2012) based on a historically outstanding paper by Ladd (1994).

4. NUSSELT NUMBER CALCULATION

The Nusselt number gives the enhancement of heat transfer by convection with respect to pure conduction. In dimensionless LB variables, it can be defined for a cylinder as

$$Nu=\frac{\nabla^*\theta\times D^*}{\theta_s-\theta_\infty}, \tag{22}$$

where $D^* = D/h$ gives the number of lattice-spacing h along the cylinder diameter D.

The calculation of the Nusselt number considers the temperature difference between the cylinder surface and the isotherms and the radial distance between these points. Figure 4 shows the isotherm lines for a flow around a cylinder with Re = 100, at the time step t = 99900.

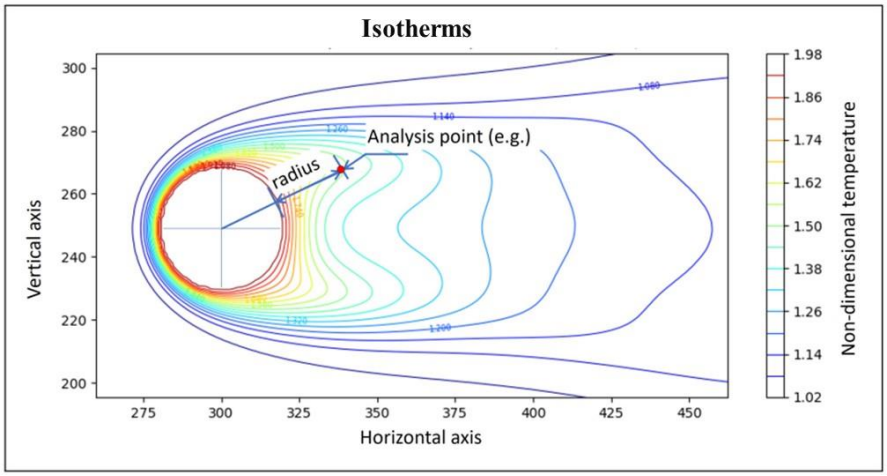

Figure 4: Isotherm lines and a random point for Nusselt number calculation for Re=100 at time step t=99900.

Due to its intrinsic cartesian nature, in LB simulation round or inclined surfaces are represented as staircases. Therefore, the isotherms close to the surface will be deformed as shown in Figure 5.

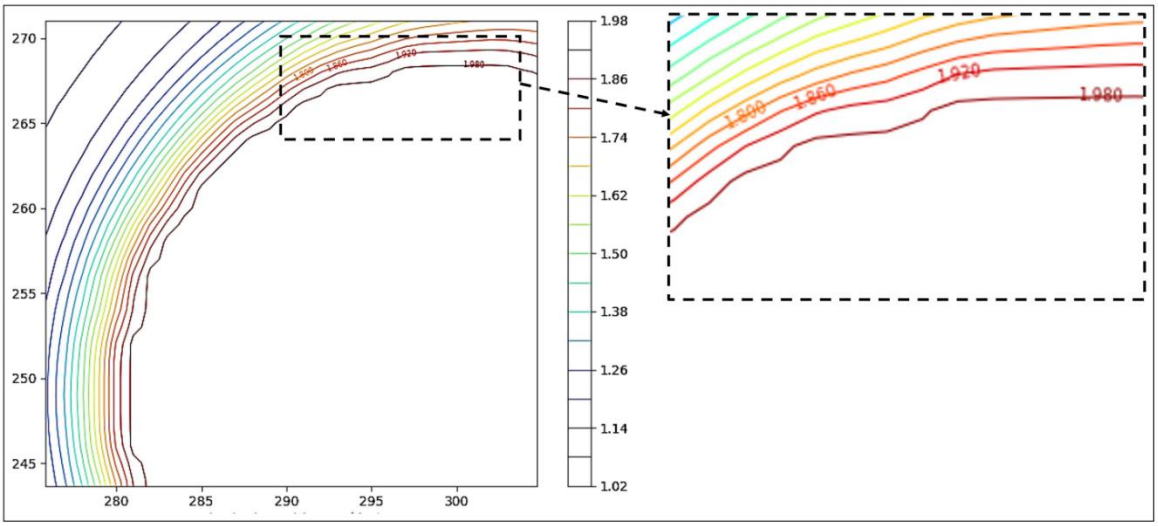

Figure 5: Isotherms close to the hot cylinder surface for Re=100

The effect of this deformation on the Nusselt number is shown in Figure 6 where the average Nusselt number is given for the isotherms from 1.5 to 1.92. From left to right, or from the colder to warm, the Nusselt number increases as the isotherm approaches the cylinder. Nevertheless, it is clearly seen that there is an abrupt increase in the Nusselt number for the isotherm $\theta = 1.92$. We attributed this singularity to the stair-case geometry of the cylinder surface and in all the subsequent calculations of the local Nusselt number we considered the isotherm $\theta = 1.86$ and its radial distance from the surface.

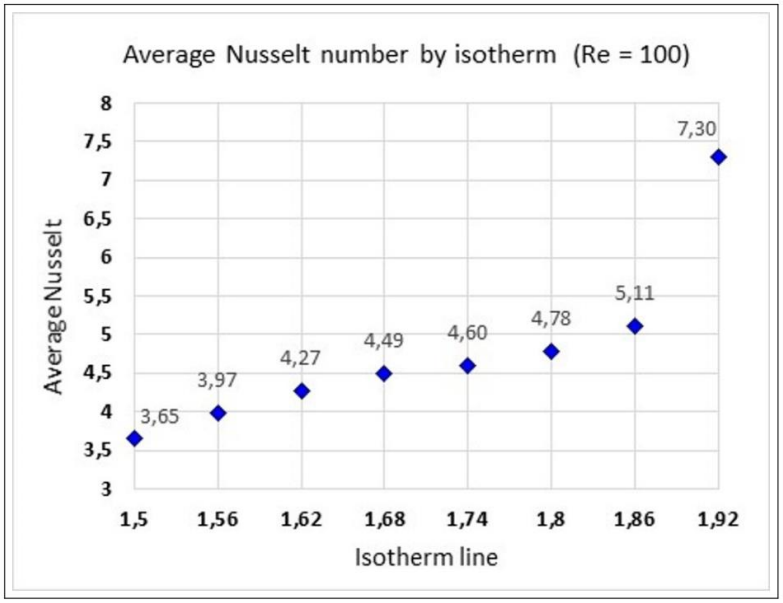

Figure 6: Average Nusselt number by isotherm for a single-cylinder with Re = 100.

5. RESULTS

In this section, the preliminary results already obtained for the simulations with a single-cylinder, are presented. Calculations were performed for Pr=0.71, with the Reynolds number varying between 10 and 120. The simulation grid is described below:

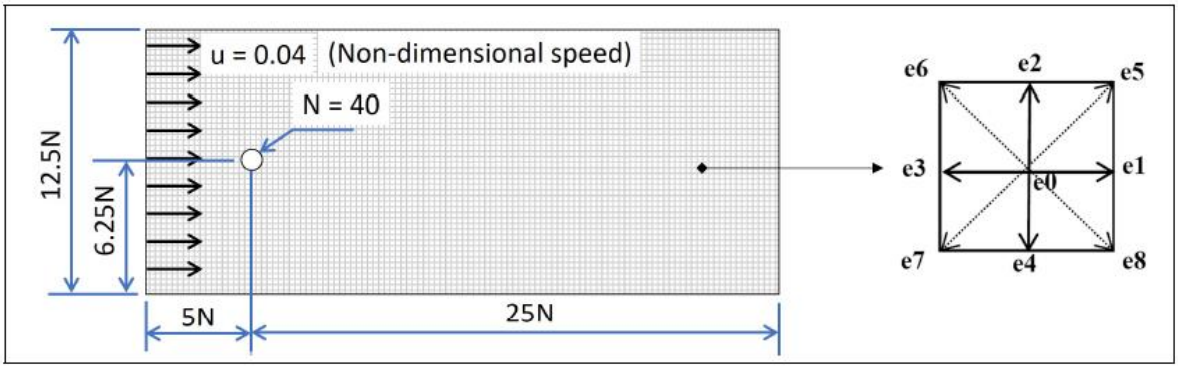

Figure 7: Simulation grid

5.1 Single cylinder

After several tests using different dimensions for the numerical domain and cylinder diameter, Figure 8 shows the scheme which appeared as the best suitable for simulating the flow and heat transfer from a single cylinder. The temperature field for the simulations with the Reynolds numbers Re=120 at the time t = 100,000 time steps is described on it. Periodic fluctuations in the temperature field are noted. As it was to be expected, there is also an increase in the temperature field on the rear surface of the cylinder, because when the cooling fluid flows past the cylinder it is heated by the cylinder's hot surface.

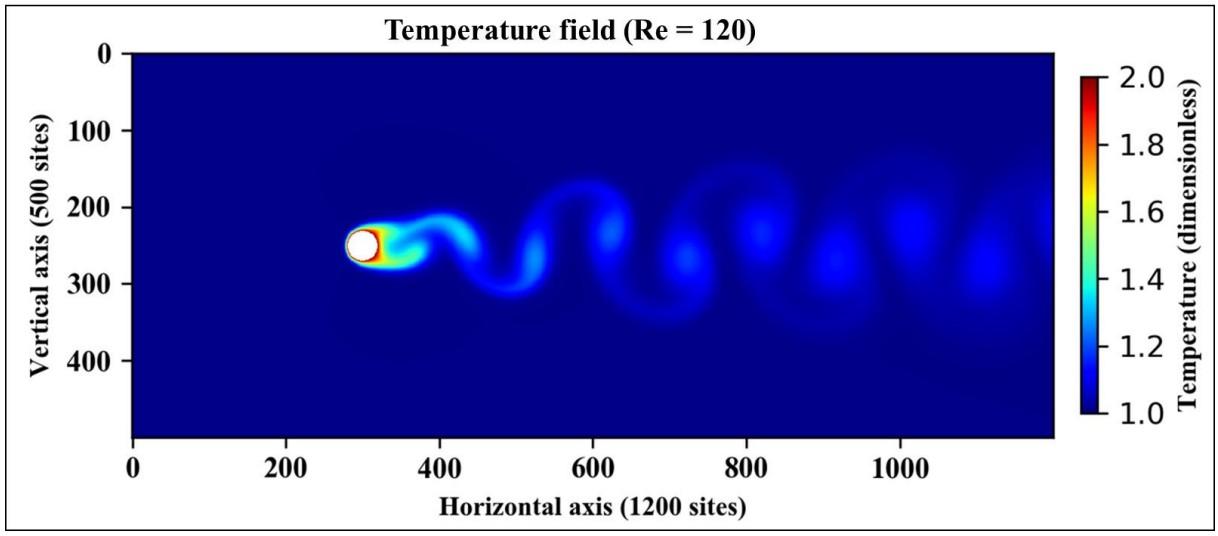

Figure 8: Temperature field for the simulations with the Reynolds numbers Re=120

Due to the periodic oscillations in the field temperature, the calculation of an average temperature field is required for obtaining the average Nusselt number. This average field for Re = 100 is shown in figure 9. Figure 10 shows the variation of the local Nusselt number with the angular coordinate θ for Re = 100 and Pr = 0.71. The Nusselt number attains its maximum value on the front stagnation point $\alpha = 0°$, where the hotter isotherms are closer to the cylinder surface and a small, but noticeable, increase on the rear stagnation region $\alpha = 180°$. It is very apparent

that the curve $Nu = f(\alpha)$ has a visible symmetric profile as it should be. This symmetry is to be noticed considering the approximation method employed in the Nu calculation, based on the location of the θ = 1.86 isotherm.

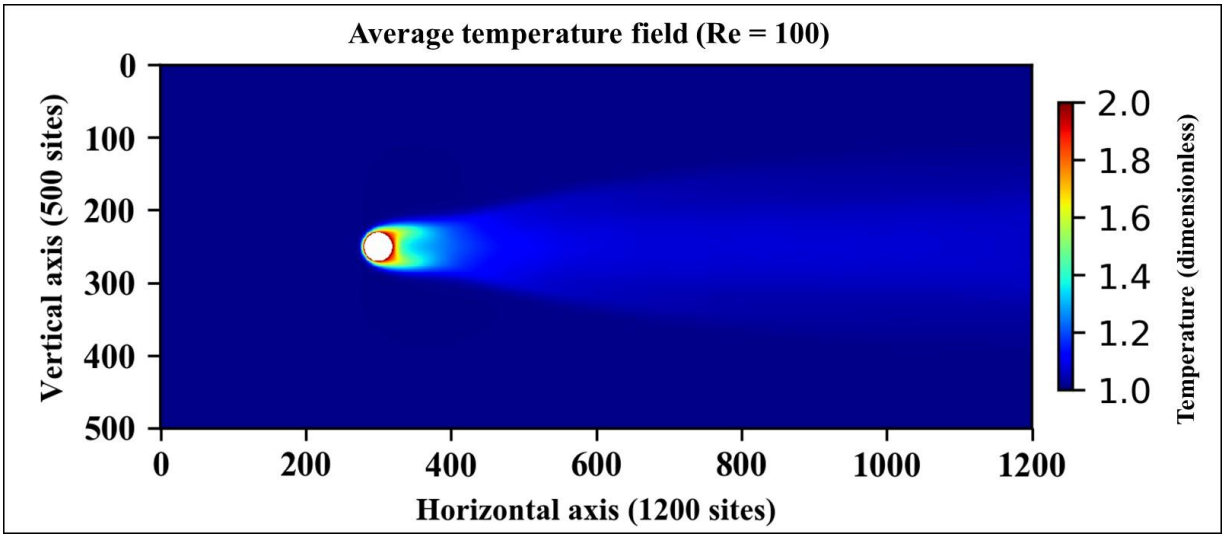

Figure 9: Average temperature field with the Reynolds numbers Re=100

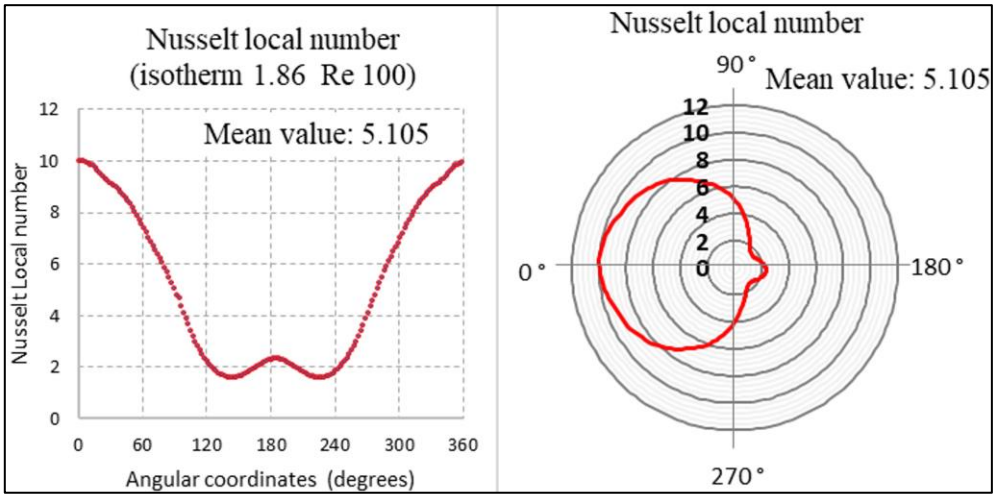

Figure 10: Local Nusselt number for a single cylinder with Re 100.

The table 1 and Fig. 11 presents the average Nusselt numbers with Re from 10 to 120 in comparison with other studies from different authors by experimental methods, where is noted a good agreement with reference values.

Table 1 - Average Nusselt number results for a single cylinder:

Author	Re10	Re20	Re40	Re60	Re80	Re100	Re120
Churchill (1977)	1.829	2.464	3.364	4.056	4.640	5.156	5.623
Hilpert (1933)	1.963	2.563	3.347	3.913	4.673	5.185	5.645
Zukauskas, A. (1987)	1.600	2.270	3.210	3.930	4.550	5.070	5.580
Average Nu from above works	1.797	2.432	3.307	3.966	4.621	5.137	5.616
Nu (present work)	1.840	2.480	3.227	3.843	4.470	5.105	5.676
Deviation (%)	2.370	1.960	-2.420	-3.110	-3.270	-0.630	1.070

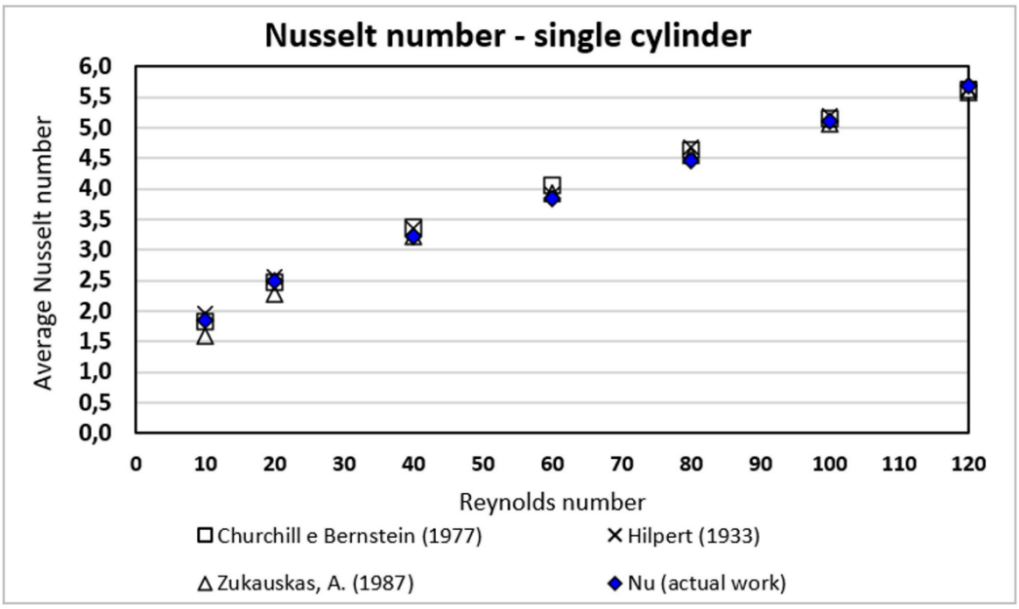

Figure 11: Local Nusselt number for a single-cylinder with Re 100.

5.2 Multiple cylinders

This section describes the heat transfer analysis for a bank of 4 cylinders in aligned and staggered layouts. The analysis is performed for Re=80 and 120. The calculations are performed using the same procedure as before for the reference isotherm θ = 1.86.

5.2.1 Bank of four aligned cylinders

The LB numerical simulation for the flow and heat transfer from a bank of four aligned cylinders was performed using the scheme shown in figure 12. The figure 13 shows the dimensionless temperature fields of the simulations in the time step = 100,000 for the aligned configuration, with Reynolds Re=80. Temperature gradients and time fluctuations due to vortex shedding were found.

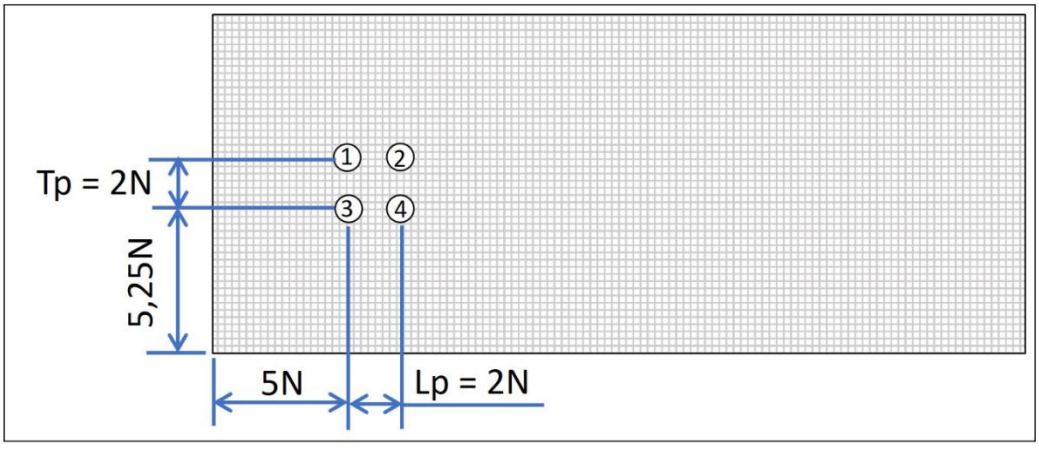

Figure 12: Simulation scheme for a bank of 4 aligned cylinders.

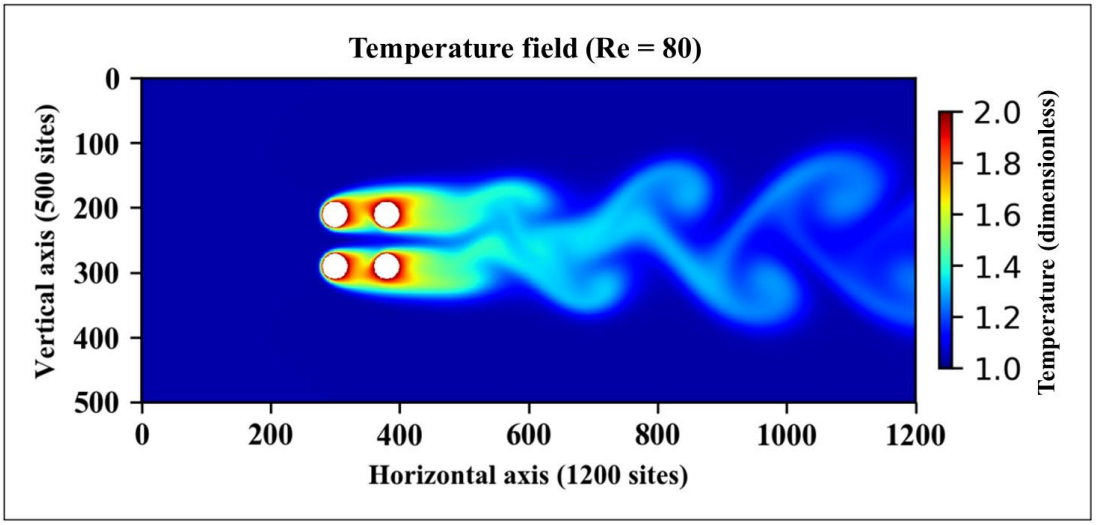

Figure 13: Temperature field for a bank of 4 aligned cylinders with Re = 80 after 100,000 time steps.

Figure 14 shows the time-averaged isotherm lines for Re = 80, detailing the region close to the cylinder surfaces and highlighting the isotherm θ = 1.86. Due to the heating process, the fluid flowing through the inner part of the bank of cylinders becomes hotter than the flow surrounding the bank. The effect of this heating process on the Nusselt number is very visible in Figure 15: the angular distribution of the Nusselt number for the lower row of cylinders appears as mirror images of the Nu angular distribution for the upper row of cylinders. This effect was to be expected considering the symmetry of the heating process. The averaged Nusselt number considering its whole angular distribution is also shown in Figure 15. Small differences due to numerical errors and to the calculation method are also to be expected. For cylinder 1, $\langle Nu \rangle$ = 4.34, against $\langle Nu \rangle$ = 4.36 for cylinder 3. For cylinder 2 $\langle Nu \rangle$ = 1.99 while $\langle Nu \rangle$ = 2.01 for cylinder 4.

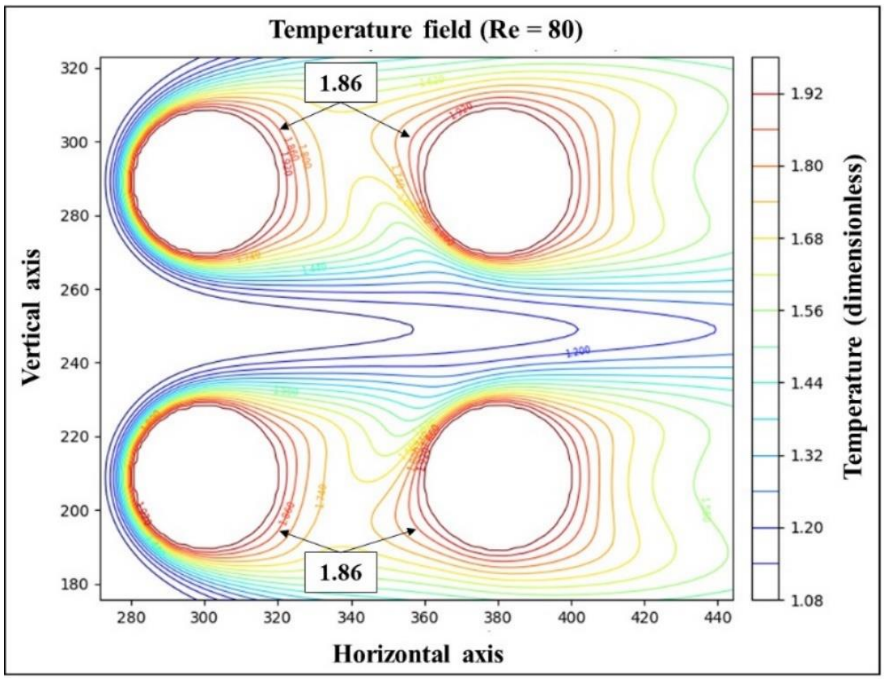

Figure 14: Averaged isotherms for a bank of 4 aligned cylinders with Re = 80

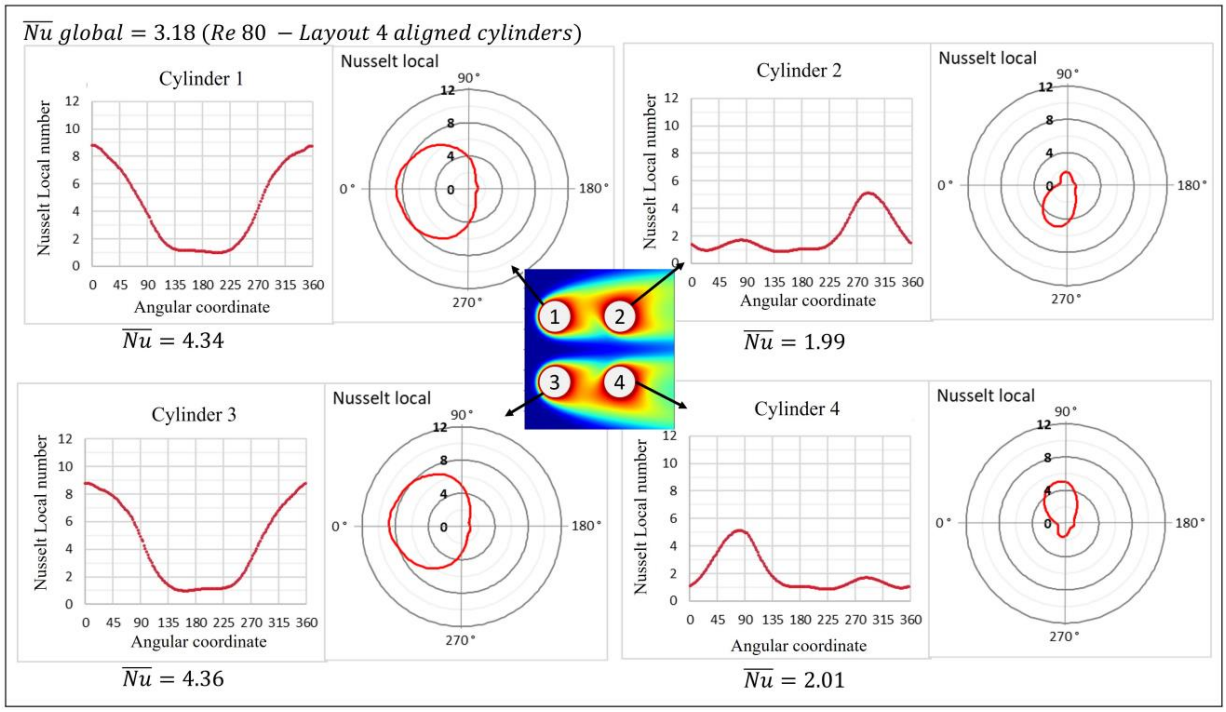

Figure 15: Nusselt local and mean values at Re = 80 for 4 aligned cylinders. Cylinder 1: (Nu) =4.34. Cylinder 2: (Nu) =1.99. Cylinder 3: (Nu) =4.36. Cylinder 4: (Nu) =2.01.

5.2.2 Bank of four staggered cylinders

The LB numerical simulation for the flow and heat transfer from a bank of four aligned cylinders was performed using the scheme shown in Figure 16. Figure 17 shows the dimensionless temperature fields in the time step = 100,000 for the staggered configuration, with Reynolds Re=80. As before, the temperature field has periodic time fluctuations due to vortex shedding are present.

Figure 18 shows the averaged isotherm lines for Re= 80 and 120 detailing the region close to the cylinders and highlighting the isotherm θ = 1.86. The system has a very visible symmetry line at y=250 l.u., cylinders 2 and 4 having the same heat transfer patterns with increased Nusselt number angular distribution when compared with the previous aligned configuration. This increase is clearly shown in Figure 19, the angular averaged Nusselt number attaining the values 4.775 for cylinder 2 and 4.771 for cylinder 4. In fact, they should be identical, and as before, this small deviation is to be attributed to numerical errors and to the calculation method that was employed. LB simulation results in an angular distribution of the Nusselt number which is perfectly symmetric for all the four cylinders. This is consistent with the symmetry of the problem and validates the LB method for this kind of problem.

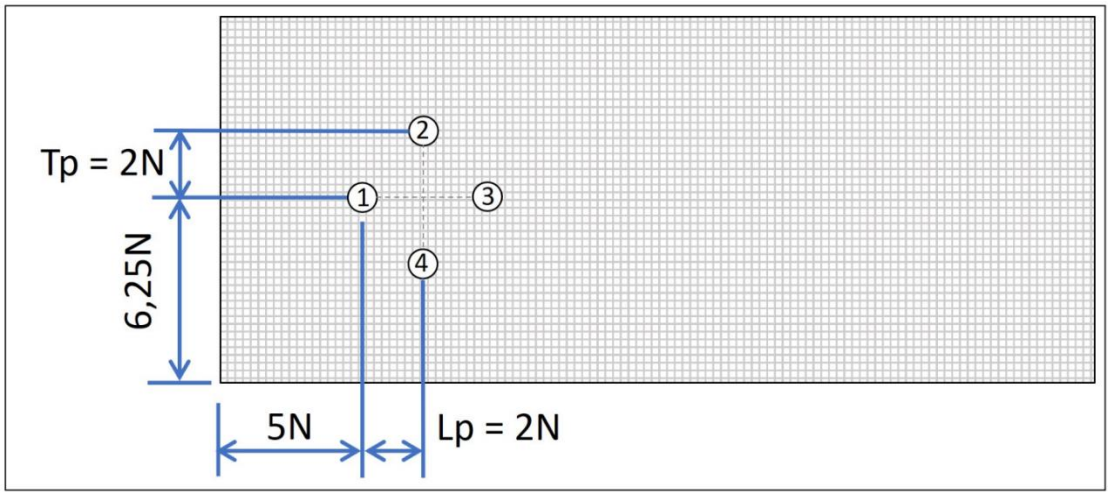

Figure 16 - Simulation scheme for a bank of four staggered cylinders.

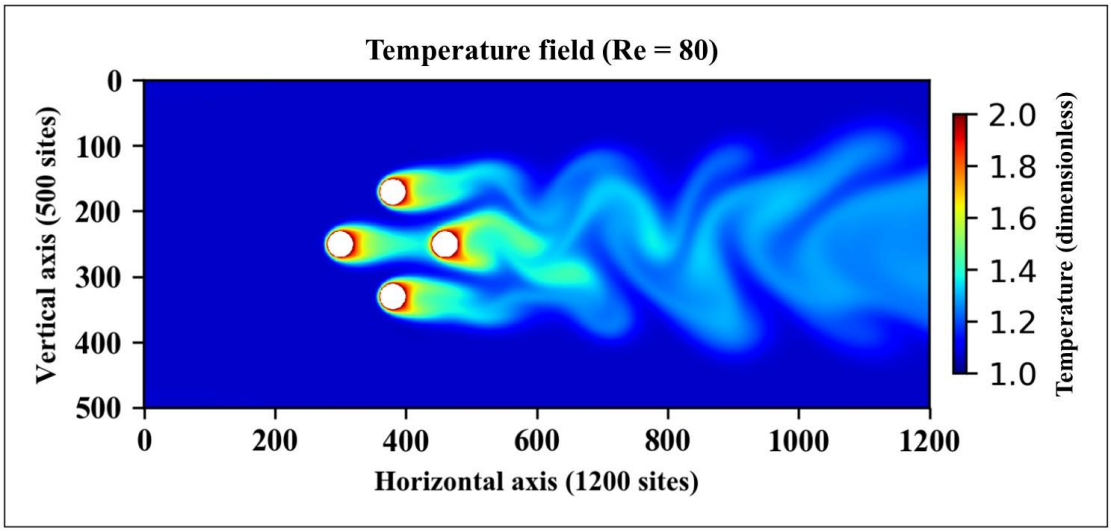

Figure 17 - Temperature field for a bank of four staggered cylinders with Re 80

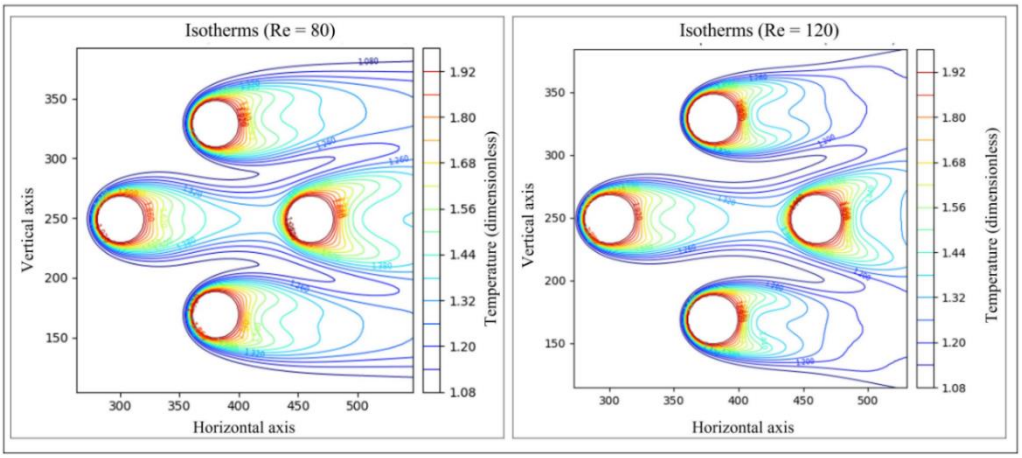

Figure 18 - Isotherms for a bank of four staggered cylinders with Re 80 and 120.

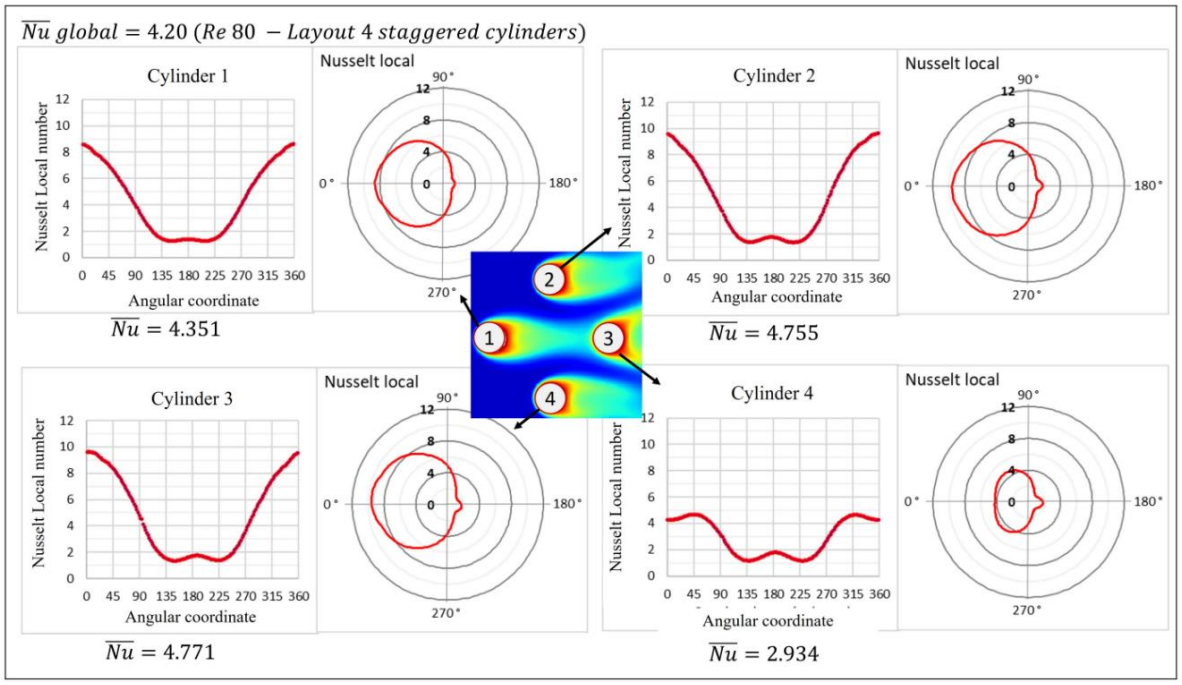

Figure 19 - Nusselt local and global for a bank of four staggered cylinders with Re 80.

The table 2 presents the average Nusselt numbers with Re 80 and 120 in comparison with other studies from different authors by experimental methods, where is noted a good agreement with reference values.

Table 2 - Global Nusselt number results for a bank of 4 cylinders:

Layout	Reference	Re80	Re120	Nu increase (%)
Aligned	Grimison (1937) – Exp.	3.31	4.28	29.3
	Zukauskas (1972) – Exp.	3.69	4.34	17.6
	Esfahani & Vasel-Be-Hagh (2012) - LBM	3.28	3.90	18.9
	Average of reference above	3.43	4.17	21.9
	Present work	3.18	3.87	21.7
	Deviation from mean reference (%)	-7.20	-7.27	
Staggered	Grimison (1937)	4.94	6.19	25.3
	Zukauskas (1972)	4.10	4.83	17.8
	Average of reference above	4.52	5.51	21.6
	Present work	4.20	5.24	24.8
	Deviation from mean reference (%)	-7.08	-4.90	

Analisyng the above results on the present work, is possible to verify an increase of 22 % and 25 % on the heat transfer coefficient for aligned and staggered layouts respectively, by increasing Reyonlods number. When comparing the same layouts and keeping the same Reynolds number, is possible to verify a higher increase by changing the layout from aligned to staggered. Table 3 below better describes:

Table 3 - Global avarage Nusselt number comparison of present work for a bank of 4 cylinders:

Re / Layout	Aligned	Staggered	Nu increase (%)
Re 80	3,18	4,2	32,1%
Re 120	3,87	5,24	35,4%
Nu increase (%)	21,7%	24,8%	-

6. CONCLUSIONS

The main purpose of this paper was to produce a comparison study of heat transfer for different layouts of a bank of cylinders. To assess the relative performance between arrangements, the LBM method for numerical simulations of flows past solid bodies was applied. The BGK standard collision operator was employed with simulation in Python language. The results are in good agreement with references available in literature from simulations performed by other authors based on CFD traditional methods. It was found deviations below 7.3 % for aligned layout and 7.08 % as a maximum difference for a bank of 4 staggered cylinders. Considering the found results, the method can be considered a fair alternative to computational simulations to preview heat transfer in different layout arrangements. When keeping same Re numbers and changing the layouts from aligned to staggered, a higher increase on Nusselt numbers is noted (32.1 and 35.4% respectively) when comparing the same layout and changing only Reynolds from 80 to 120, where an increase of 21.7 and 24.8% are respectively found. This means that during the design stage of bank of cylinders, as an example for heat exchangers, a choice on the tube layout arrangements would be more interesting than increasing a forced flow over heat exchangers.

Credit authorship contribution statement

E. M. Porto: Numerical simulations, Comparative analysis, Bibliographic survey and analysis of previous works. **S. H. Och***: Conceptualization of this study, Methodology. **P.C. Philippi**: Conceptualization of this study, Methodology, writing- Original draft preparation

7. REFERENCES

Bazarin, R., Philippi, P., Randles, A., Hegele, L., 2021. Moments-based method for boundary conditions in the lattice Boltzmann framework: A comparative analysis for the lid-driven cavity flow. Computers Fluids, 105142 URL: https://linkinghub.elsevier.com/retrieve/pii/S0045793021002772, doi:10.1016/j.compfluid.2021.105142.

Bhatnagar, P.L., Gross, E.P., Krook, M., 1954. A Model for Collision Processes in Gases. I. Small Amplitude Processes in Charged and Neutral

Chen, S., Doolen, G.D., 1998. Lattice Boltzmann Method For Fluid Flows. Annual Reviews of Fluid Mechanics 30, 329–364. doi:10.1007/978-0-85729-455-5.

Churchill, S., & Bernstein, M. (1977). J. Heat Transfer, 99 - 300, .

Esfahani, J., & Vasel-Be-Hagh, A. (2012). LB simulation of heat transfer in flow past a of four isothermal cylinders. *Comptes Rendus Mecanique*, Vol 340 pp 526–535 URL: https://linkinghub.elsevier.com/retrieve/pii/S1631072112000721, doi:10.1016/j.crme. 2012.03.011.

Grimison, E. D. (1937). Trans. ASME, . 59 - 583

Hilpert, R. (1933). Forsch. Geb. Ingenieurwes, 4 - 215.

He, X., Chen, S., Doolen, G.D., 1998. A Novel Thermal Model for the Lattice Boltzmann Method in Incompressible Limit. Journal of Computational Physics 146, 282–300. URL: http://linkinghub.elsevier.com/retrieve/pii/S0021999198960570, doi:10.1006/jcph.1998.6057.

He, X., Luo, L.S., 1997. Theory of the lattice Boltzmann method: From the Boltzmann equation to the lattice Boltzmann equation. Physical Review E 56, 6811–6817. URL: http://link.aps.org/doi/10.1103/PhysRevE.56.6811, doi:10.1103/PhysRevE.56.6811.

Hsu, L.C., Liang, C.W., 2021. Heat Transfer in Flow Past Two Cylinders in Tandem and Enhancement with a Slit. Energies 14, 308. URL:https://www.mdpi.com/1996-1073/14/2/308, doi:10.3390/en14020308.

Ladd, A.J.C., 1994. Numerical simulations of particulate suspensions via a discretized Boltzmann equation. Part 1. Theoretical foundation. Journal of Fluid Mechanics 271, 285. URL: http://www.journals.cambridge.org/abstract_S0022112094001771, doi:10.1017/S0022112094001771.

Sayehvand, H.O., Yari, S., Basiri, P., 2018. Numerical study of forced convection heat transfer over three cylinders in staggered arrangement immersed in porous media. Thermal Science 22, 467–475. URL: http://www.doiserbia.nb.rs/Article.aspx?ID=0354-98361600249S, doi:10.2298/TSCI150808249S.

Surmas, R., Dos Santos, L.O.L., Philippi, P.P.C., 2004. Lattice Boltzmann simulation of the flow interference in bluff body wakes. Future Generation Computer Systems 20, 951–958. URL: http://www.sciencedirect.com/science/article/pii/S0167739X0300267X, doi:10.1016/j.future.2003.12.007.

Zhang, T., Shi, B., Guo, Z., Chai, Z., Lu, J., 2012. General bounce-back scheme for concentration boundary condition in the lattice-Boltzmann method. Physical Review E 85, 016701. URL: https://link.aps.org/doi/10.1103/PhysRevE.85.016701, doi:10.1103/PhysRevE. 85.016701.

Zhou, X., Dong, B., Chen, C., Li, W., 2019. A thermal LBM-LES model in body-fitted coordinates: Flow and heat transfer around a circular cylinder in a wide Reynolds number range. International Journal of Heat and Fluid Flow 77, 113–121. URL: https://linkinghub.elsevier.com/ retrieve/pii/S0142727X19300165, doi:10.1016/j.ijheatfluidflow.2019.04.001.

Zou, Q., He, X., 1997. On pressure and velocity boundary conditions for the lattice Boltzmann BGK model. Physics of Fluids 9, 1591–1598. URL: http://arxiv.org/abs/comp-gas/9611001%0Ahttp://dx.doi.org/10.1063/1.869307http://aip.scitation.org/doi/10.1063/1.869307, arXiv:9611001.

Zu, Y., Yan, Y., Shi,W., Ren, L., 2008. Numerical method of lattice Boltzmann simulation for flow past a rotating circular cylinder with heat transfer. International Journal of Numerical Methods for Heat Fluid Flow 18, 766–782. URL:https://www.emerald.com/insight/content/doi/10.1108/09615530810885560/full/html, doi:10.1108/09615530810885560.

Zukauskas, A. (1972). Heat Transfer from Tubes in Cross Flow. Em J. P. Hartnett , & T. F. Irvine, Advances in Heat Transfer (p. Vol 8). New York: Academic Press.

Zukauskas, A. (1987). Convective Heat Transfer in Cross Flow. Em R. K. S. Kakac, Handbook of Single-Phase Convective Heat Transfer in Cross Flow. New York

8. THE RESPONSIBILITY NOTICE

The author(s) is (are) the only responsible for the printed material included in this paper.